Journal of Advances in Modeling Earth Systems

Supporting Information for

New features and enhancements in Community Land Model (CLM5) snow albedo modeling: description, sensitivity, and evaluation

Cenlin He[1], Mark Flanner[2], David M. Lawrence[1], Yu Gu[3]

1. National Center for Atmospheric Research (NCAR), Boulder, CO, USA
2. University of Michigan Ann Arbor, MI, USA
3. University of California Los Angeles, CA, USA

Correspondence to: Cenlin He (cenlinhe@ucar.edu)

Content of this file:

Figures S1 to S16

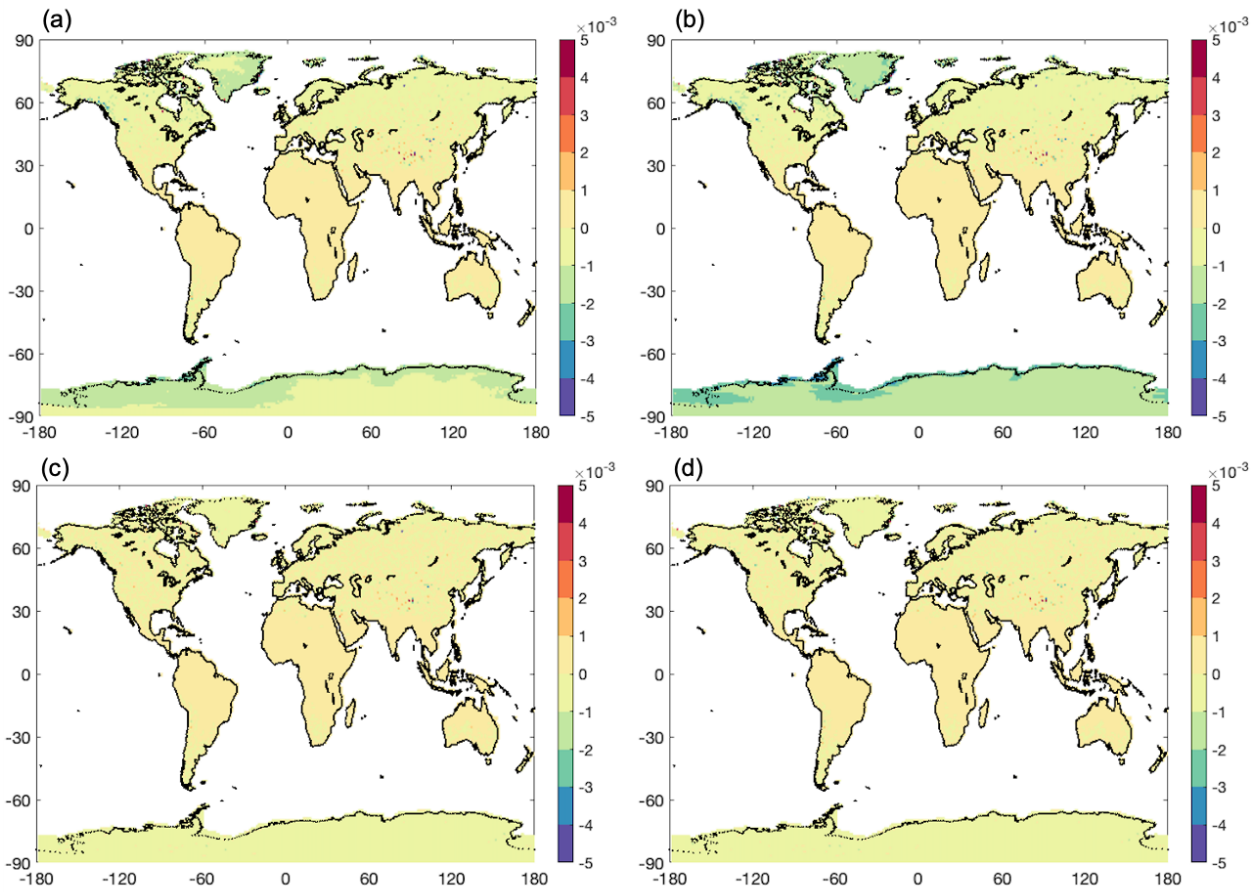

Figure S1. 5-year (2006-2010) annual mean effects of updated ice optical properties (i.e., differences between simulations using the Picard et al. (2016) and Warren and Brandt (2008) visible ice refractive indices): (a) difference for direct-beam visible snow albedo, (b) difference for diffuse visible snow albedo, (c) difference for direct-beam NIR snow albedo, (d) difference for diffuse NIR snow albedo.

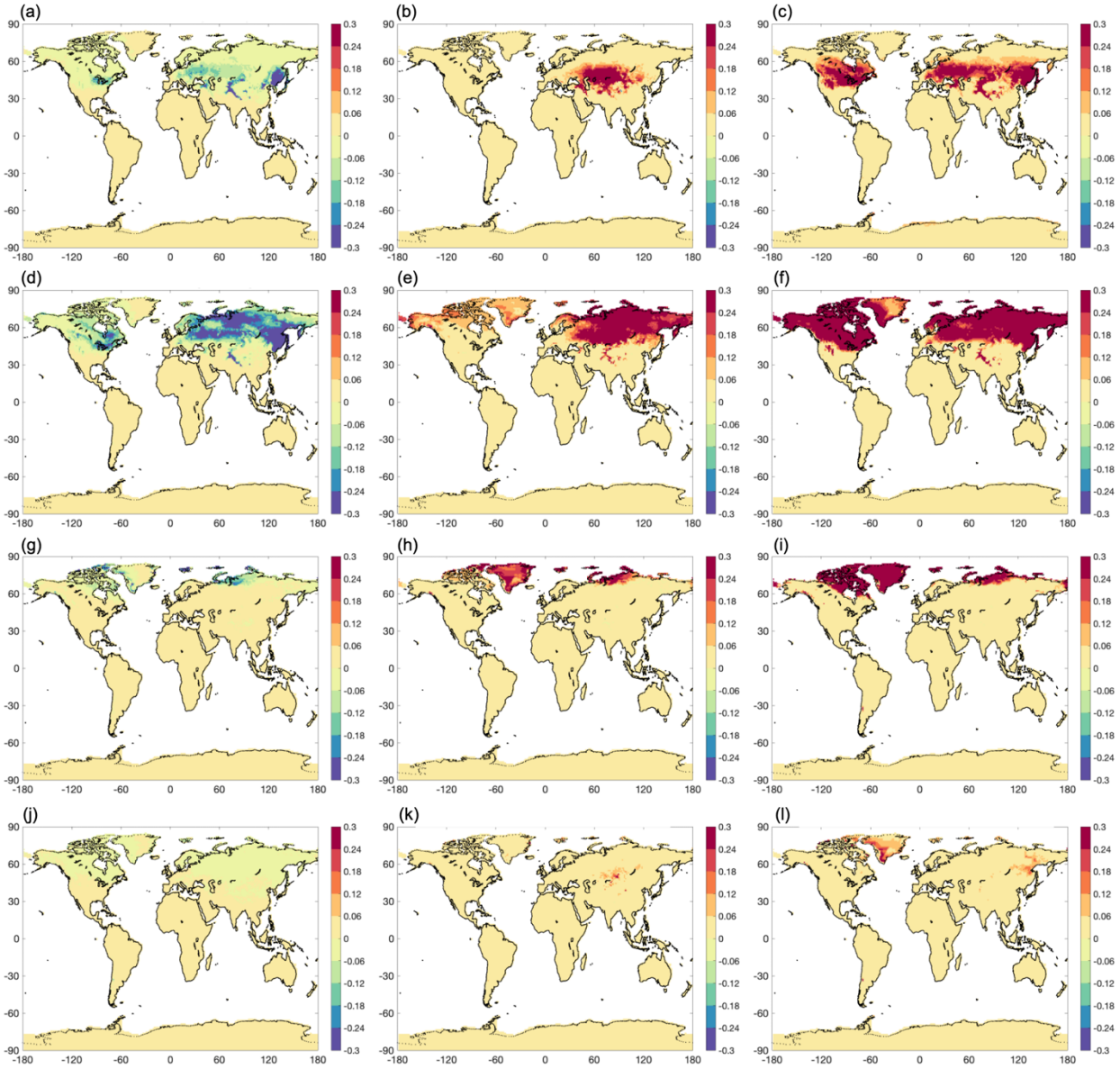

Figure S2. 5-year (2006-2010) all-sky seasonal mean effects of updated aerosol optical properties (i.e., differences between simulations using the Flanner et al. (2021) and Flanner et al. (2007) data). First column: difference for BC-induced snow albedo forcing (W m^{-2}); second column: difference for dust-induced snow albedo forcing (W m^{-2}); third column: difference for OC-induced snow albedo forcing (W m^{-2}). First row: winter (December-January-February); second row: spring (March-April-May); third row: summer (June-July-August); fourth row: fall (September-October-November).

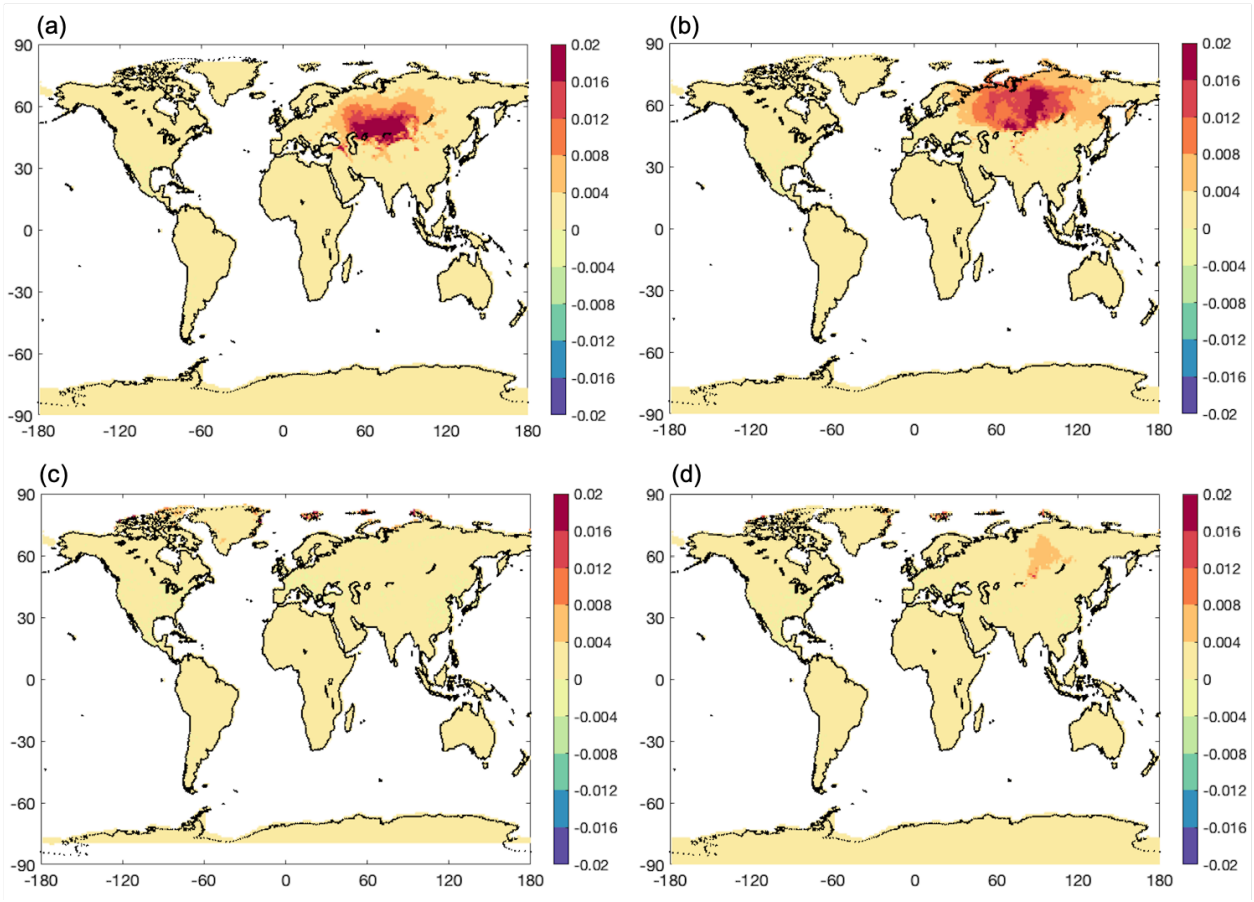

Figure S3. 5-year (2006-2010) all-sky seasonal mean effects of different dust types (i.e., differences between simulations using Greenland dust and Colorado dust) on snow-covered ground albedo reduction caused by dust: (a) winter (December-January-February), (b) spring (March-April-May), (c) summer (June-July-August), (d) fall (September-October-November).

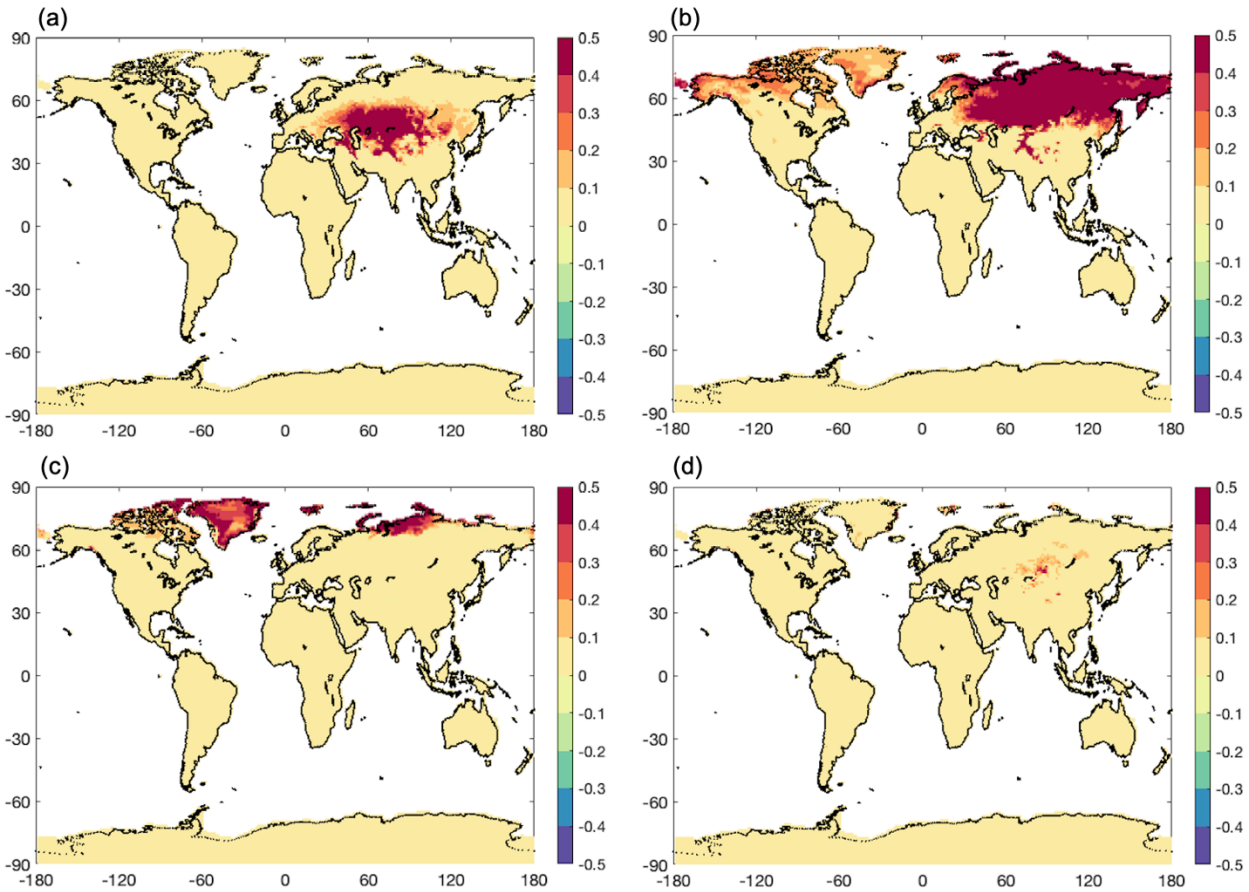

Figure S4. 5-year (2006-2010) all-sky seasonal mean effects of different dust types (i.e., differences between simulations using Greenland dust and Colorado dust) on dust-induced snow albedo forcing (W m^{-2}): (a) winter (December-January-February), (b) spring (March-April-May), (c) summer (June-July-August), (d) fall (September-October-November).

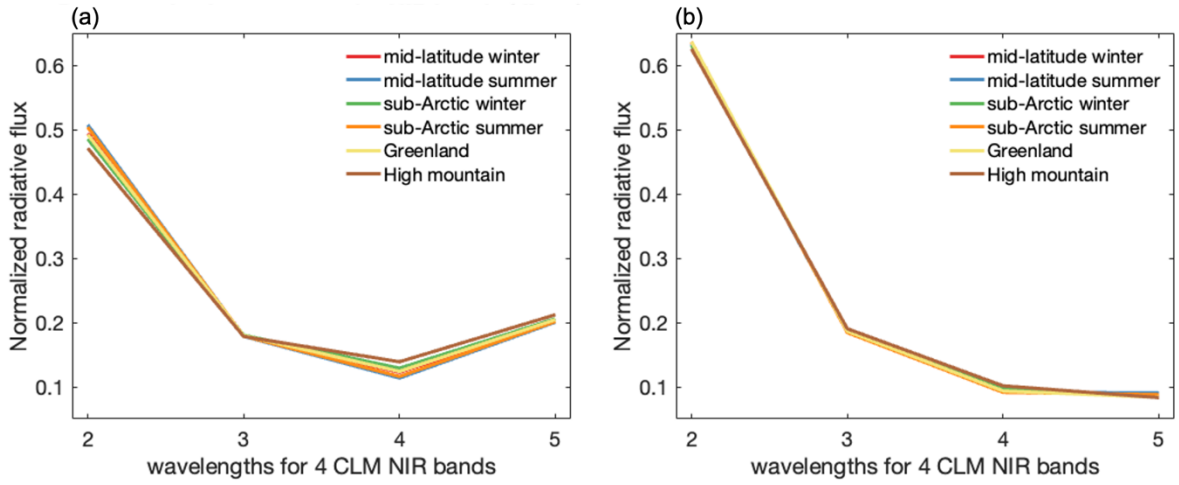

Figure S5. Normalized downward solar radiative flux spectra for six different atmospheric conditions at the four CLM near-infrared (NIR) bands for (a) direct and (b) diffuse radiation.

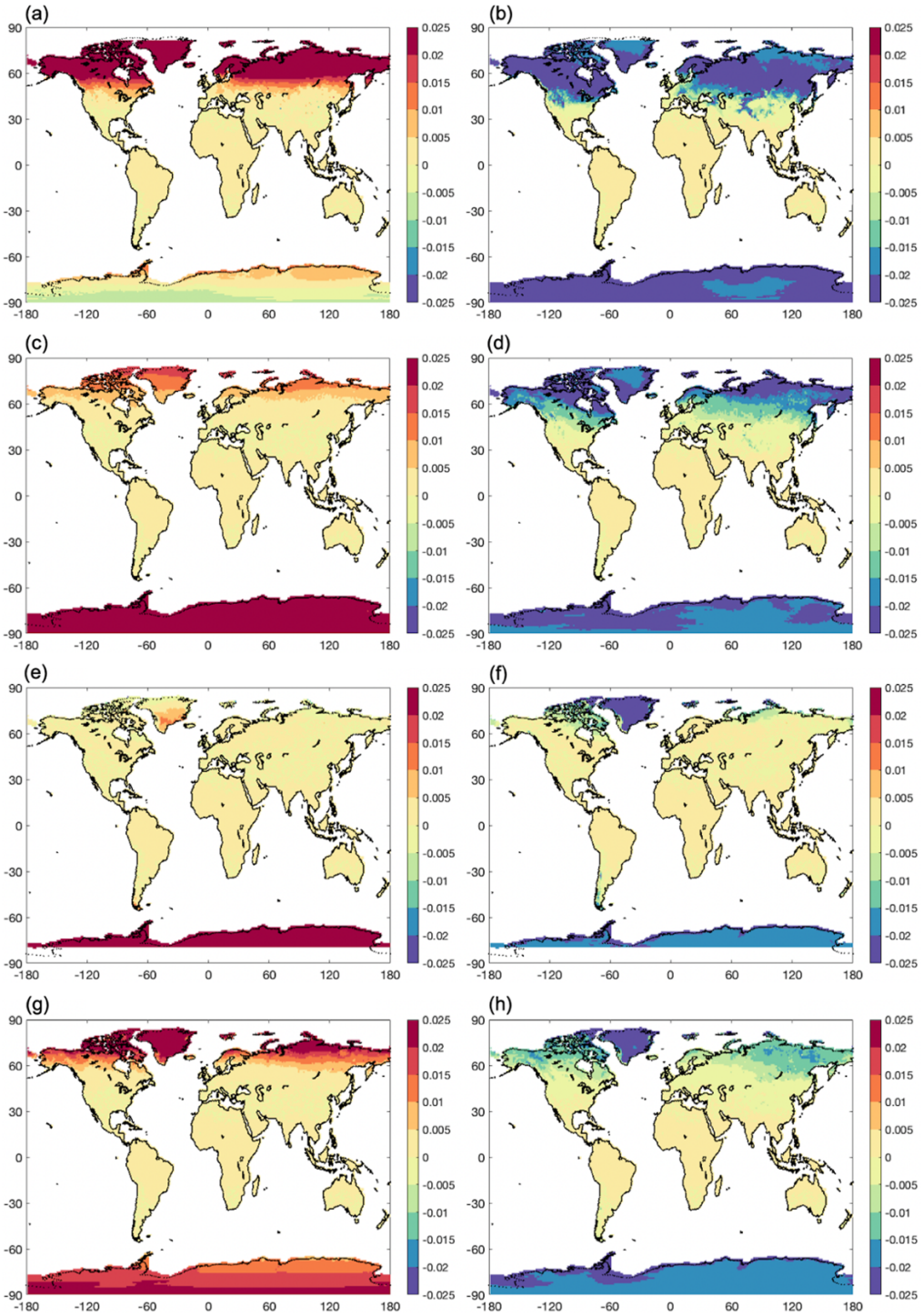

Figure S6. 5-year (2006-2010) seasonal mean effects of updated snow radiative transfer solvers (i.e., differences between simulations using the adding-doubling and Toon et al. (1989) solvers) on NIR snow albedo. First column: difference under direct radiation; second column: difference under diffuse radiation. First row: winter (December-January-February); second row: spring (March-April-May); third row: summer (June-July-August); fourth row: fall (September-October-November).

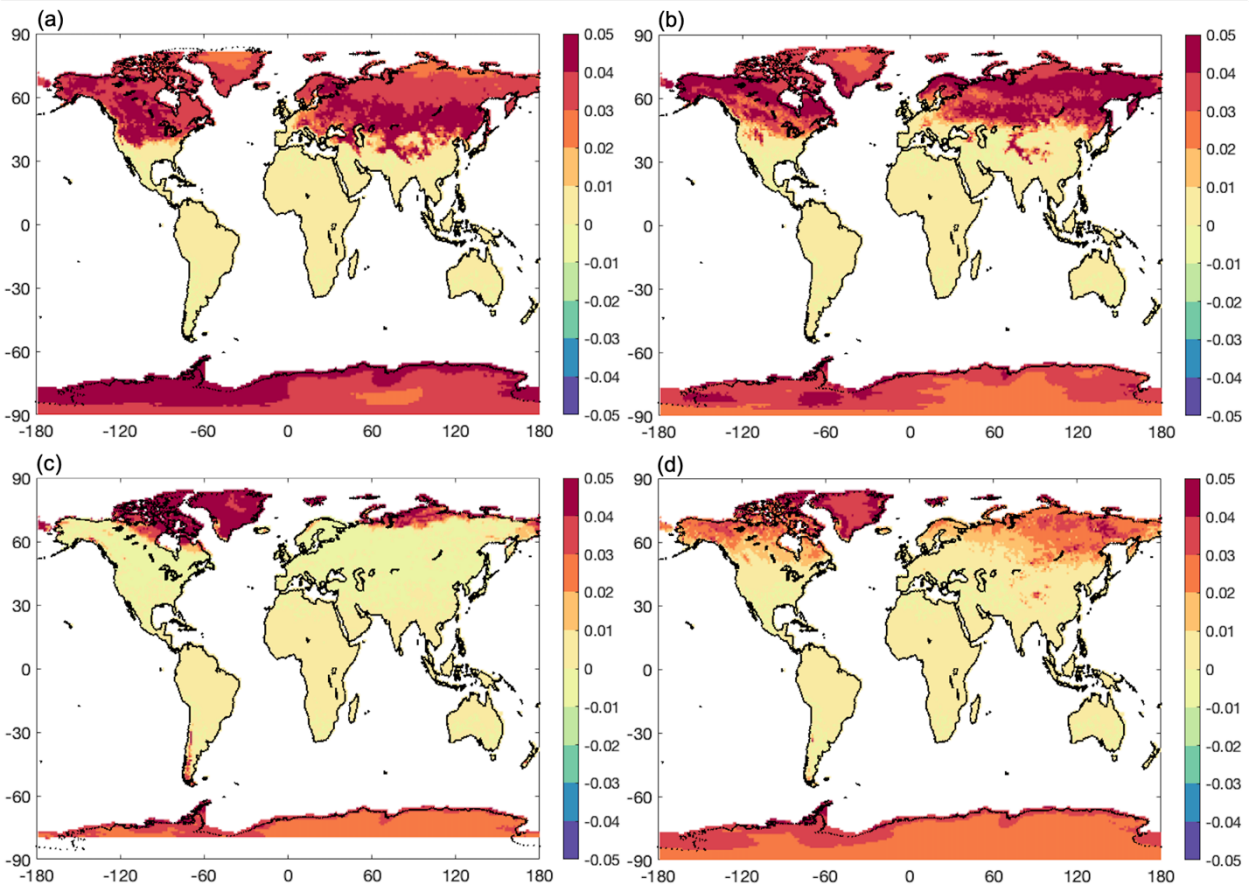

Figure S7. 5-year (2006-2010) all-sky annual mean effects of nonspherical snow grain (i.e., differences between simulations using fractal snowflake and snow sphere) on broadband snow albedo: (a) winter (December-January-February), (b) spring (March-April-May), (c) summer (June-July-August), (d) fall (September-October-November).

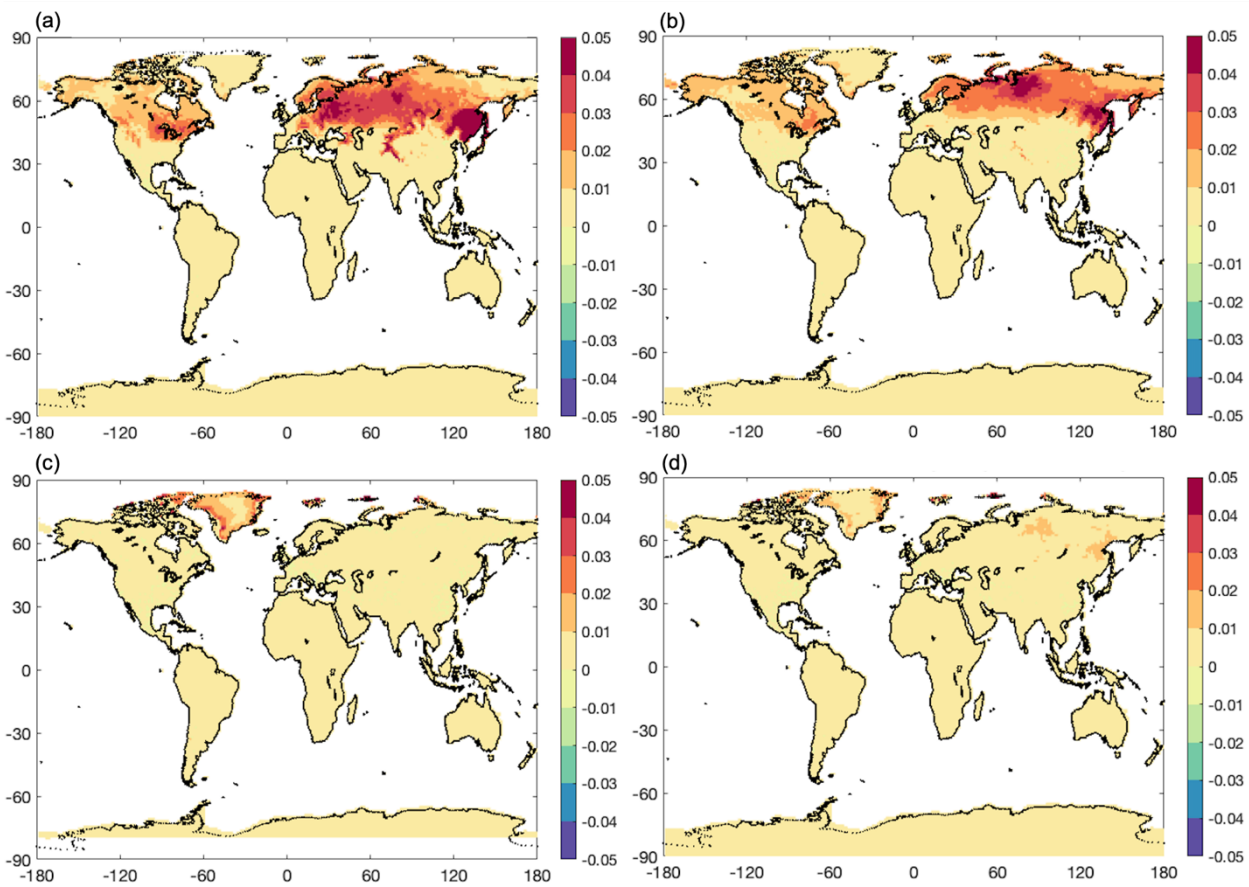

Figure S8. 5-year (2006-2010) all-sky annual mean effects of BC-snow internal mixing (i.e., differences between simulations using BC-snow internal mixing and external mixing) on BC-induced snow ground albedo reduction: (a) winter (December-January-February), (b) spring (March-April-May), (c) summer (June-July-August), (d) fall (September-October-November).

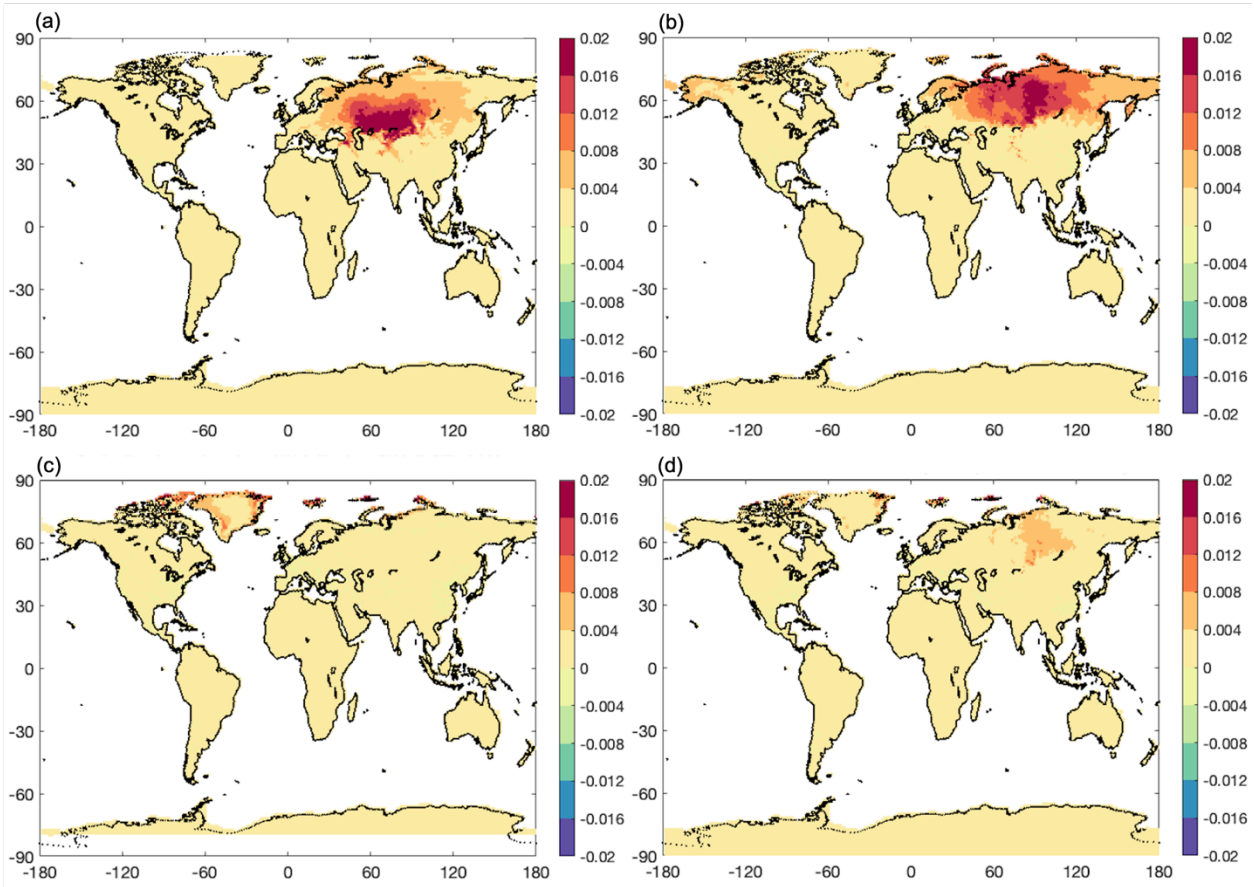

Figure S9. 5-year (2006-2010) all-sky annual mean effects of dust-snow internal mixing (i.e., differences between simulations using dust-snow internal mixing and external mixing) on dust-induced snow ground albedo reduction: (a) winter (December-January-February), (b) spring (March-April-May), (c) summer (June-July-August), (d) fall (September-October-November).

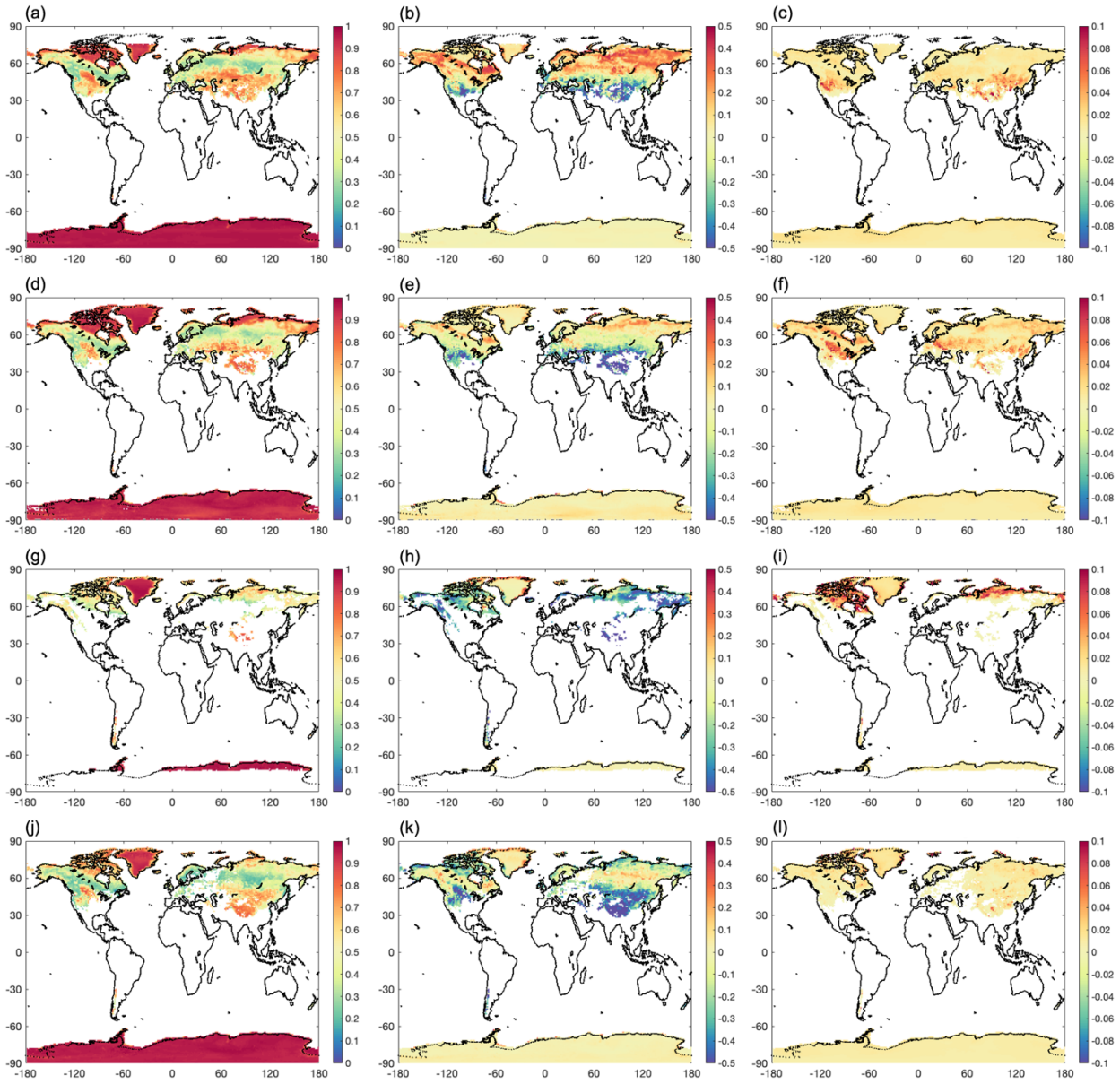

Figure S10. Comparison between MODIS and model simulations of 5-year (2006-2010) seasonal mean white-sky visible surface albedo for 100% snow cover pixels. First column: MODIS observations; second column: default CLM baseline bias; third column: difference between new and default CLM baseline simulations. First row: winter (December-January-February); second row: spring (March-April-May); third row: summer (June-July-August); fourth row: fall (September-October-November).

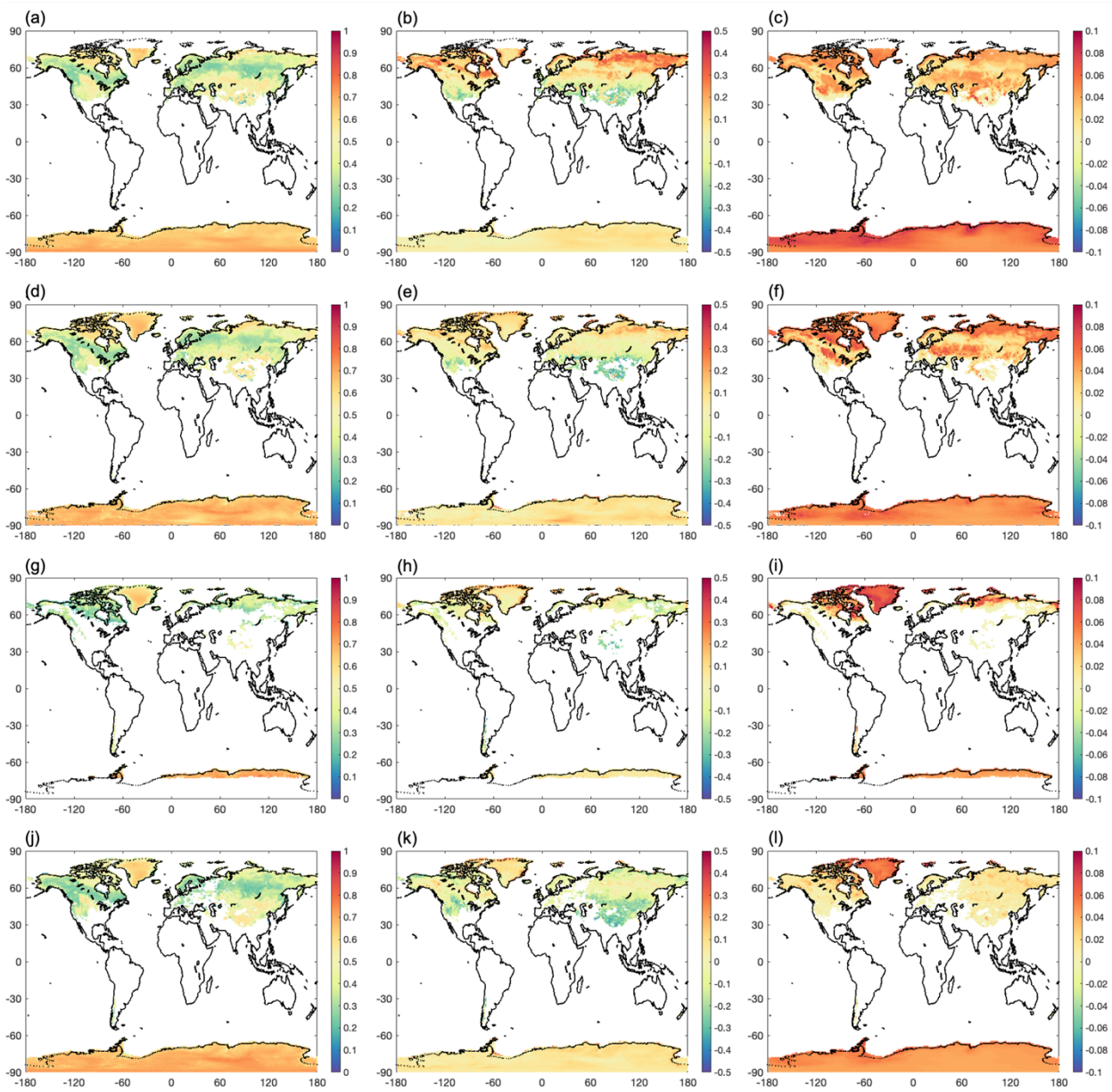

Figure S11. Same as Figure S10, but for the white-sky NIR band.

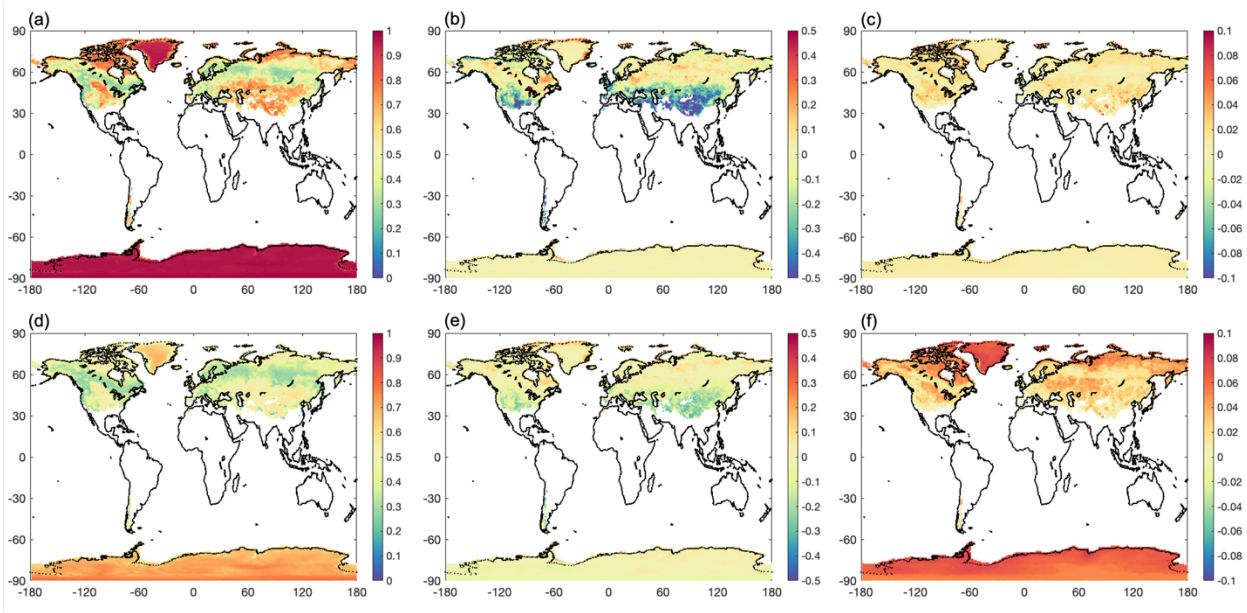

Figure S12. Comparison between MODIS and model simulations of 5-year (2006-2010) annual mean black-sky surface albedo for 100% snow cover pixels. First column (a, d): MODIS observations; second column (b, e): default CLM baseline bias; third column (c, f): difference between new and default CLM baseline simulations. First row (a, b, c): visible band; second row (d, e, f): NIR band.

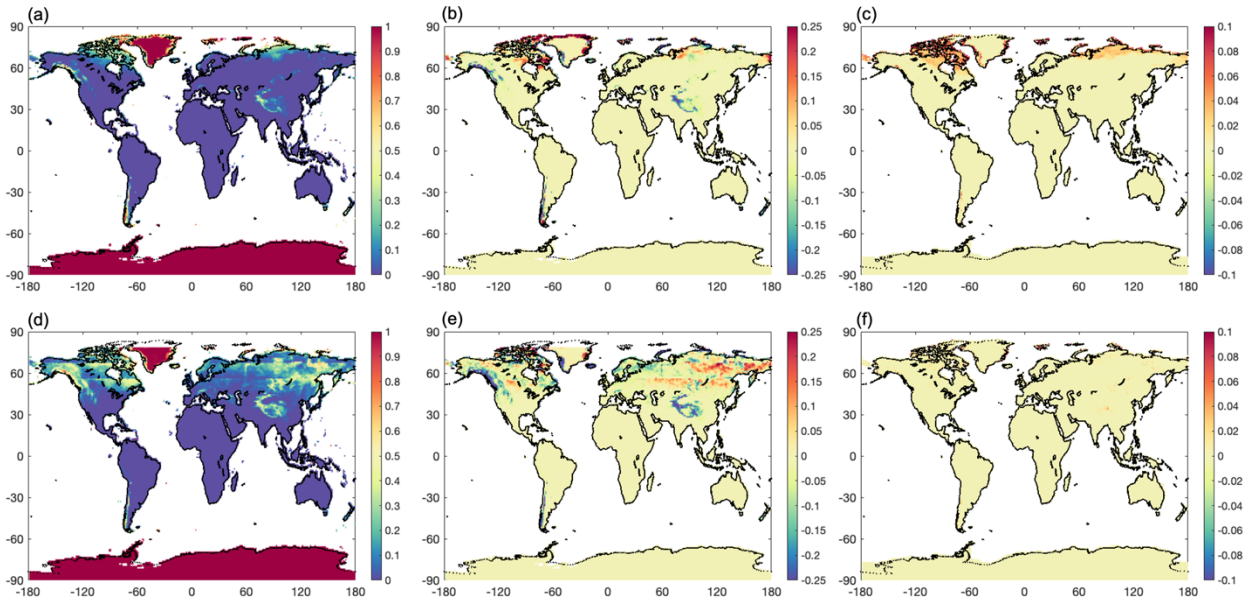

Figure S13. Comparison between MODIS and model simulations of 5-year (2006-2010) seasonal mean snow cover fraction. First column (a, d): MODIS observations; second column (b, e): default CLM baseline bias; third column (c, f): difference between new and default CLM baseline simulations. First row (a, b, c): summer (June-July-August); second row (d, e, f): fall (September-October-November).

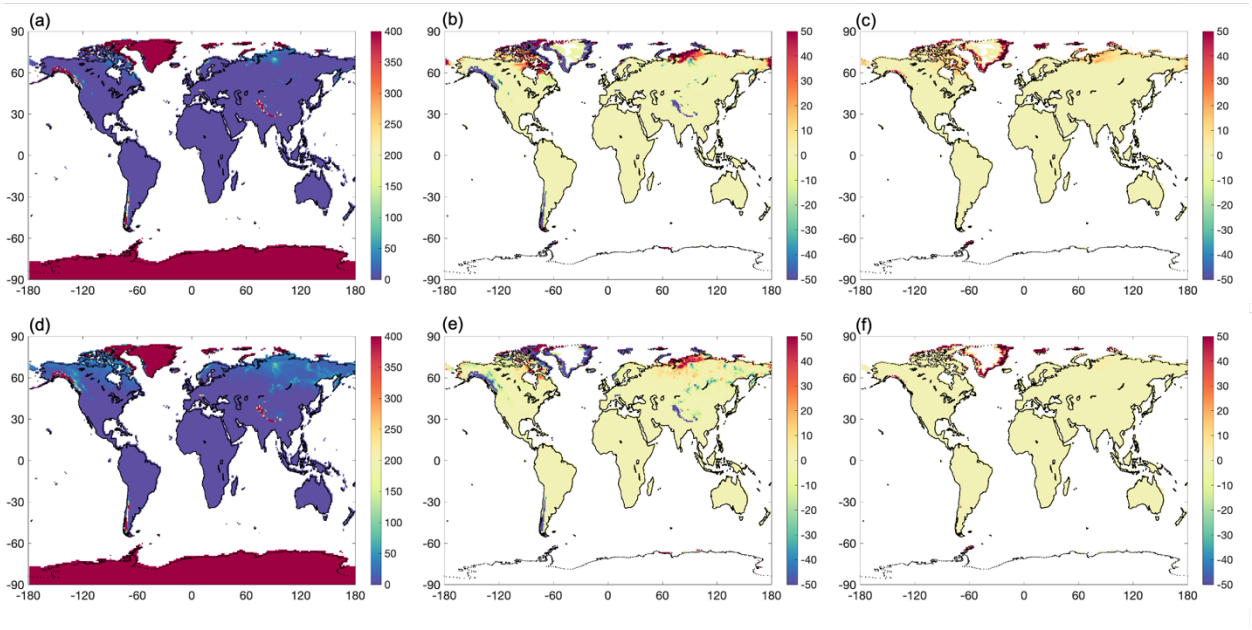

Figure S14. Comparison between ERA-5 and model simulations of 5-year (2006-2010) seasonal mean SWE (mm). First column (a, d): ERA-5 data; second column (b, e): default CLM baseline bias; third column (c, f): difference between new and default CLM baseline simulations. First row (a, b, c): summer (June-July-August); second row (d, e, f): fall (September-October-November).

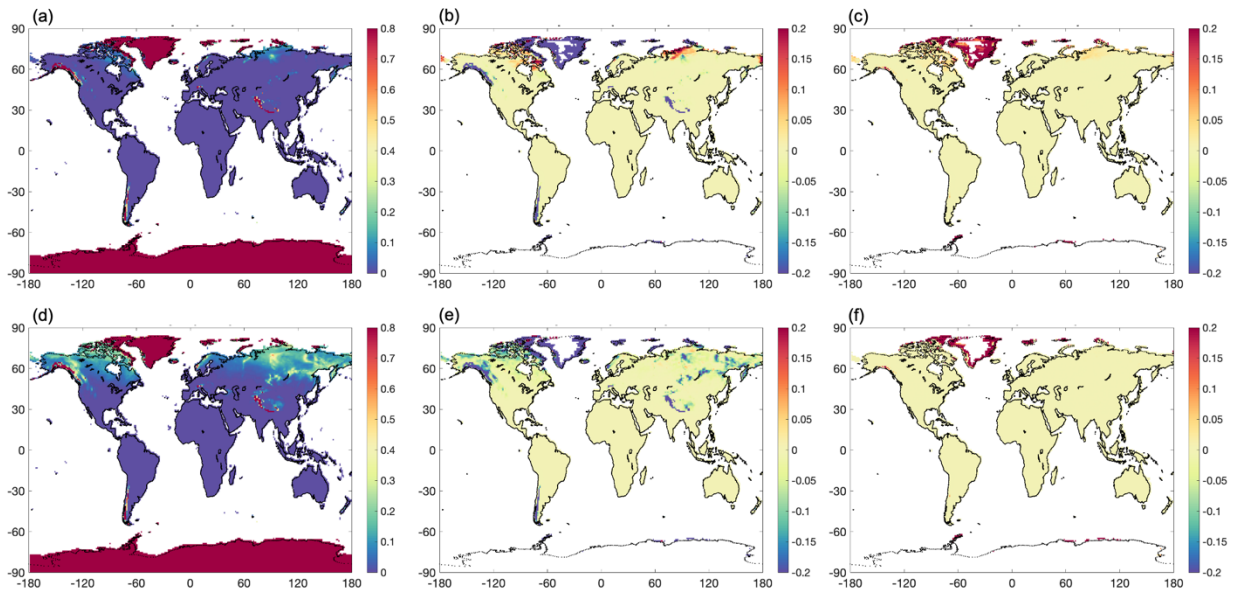

Figure S15. Same as Figure 14, but for snow depth (m) comparison between ERA-5 and model simulations.

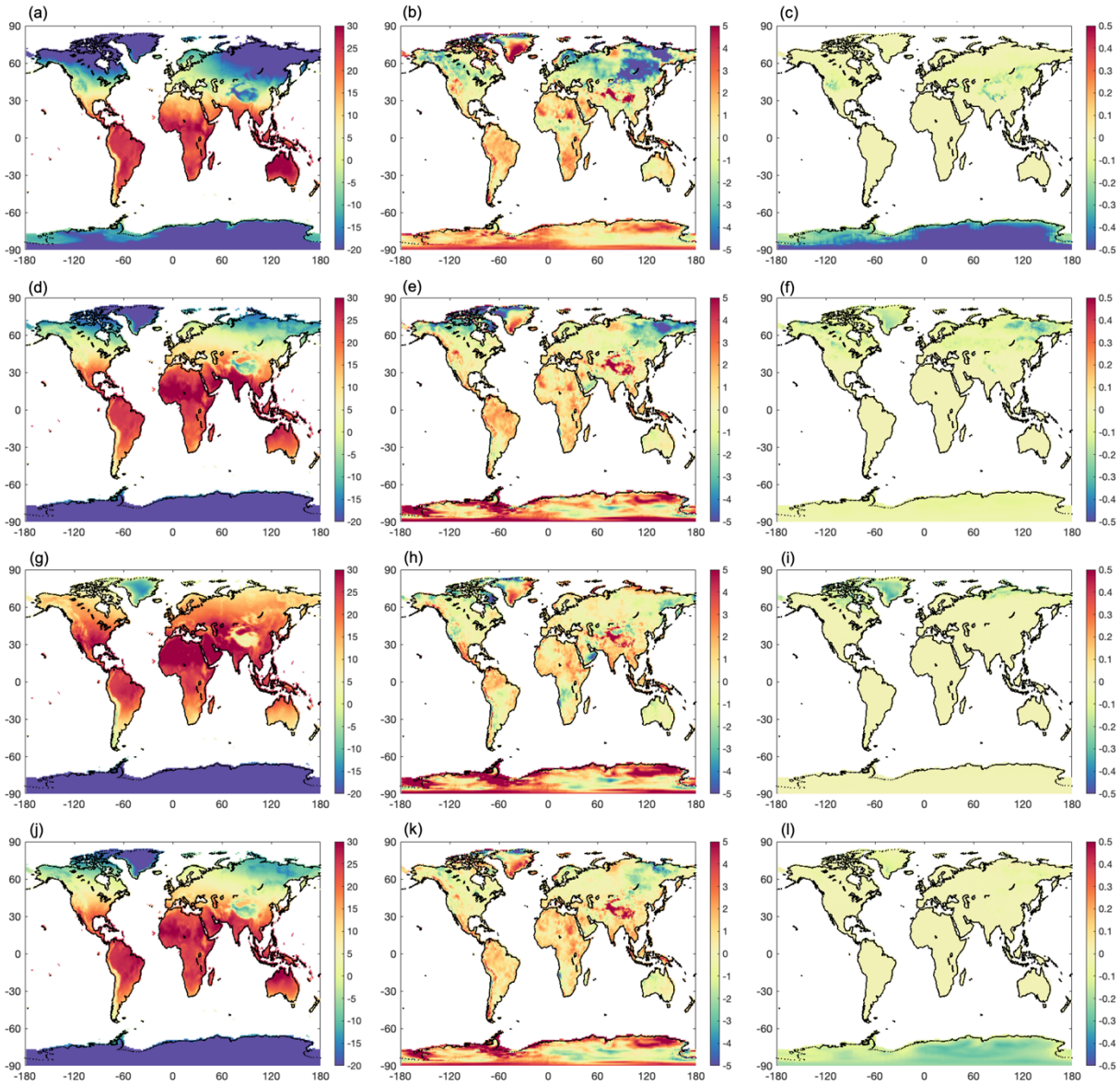

Figure S16. Comparison between ERA-5 and model simulations of 5-year (2006-2010) seasonal mean 2-m surface temperature (°C). First column (a, d, g, j): ERA-5 data; second column (b, e, h, k): default CLM baseline bias; third column (c, f, i, l): difference between new and default CLM baseline simulations. First row (a, b, c): winter (December-January-February); second row (d, e, f): spring (March-April-May); third row (g, h ,i): summer (June-July-August); fourth row (j, k, l): fall (September-October-November).